Available online at www.sciencedirect.com
ScienceDirect
Tetrahedron: Asymmetry
Tetrahedron: *Asymmetry* 17 (2006) 3158–3162

Energy barrier determination of enantiomerization of chiral 3,4-dihydro-1,2,4-benzothiadiazine 1,1-dioxide type compounds by enantioselective stopped-flow HPLC

Giuseppe Cannazza,[a,*] Daniela Braghiroli,[a] Piera Iuliani[b] and Carlo Parenti[a]

[a]*Dipartimento di Scienze Farmaceutiche, Università degli Studi di Modena e Reggio Emilia, Via Campi 183, 4100 Modena, Italy*
[b]*Dipartimento di Scienze del Farmaco, Università degli Studi 'G. d'Annunzio' Chieti-Pescara, Via dei Vestini, 66100 Chieti, Italy*

Received 11 October 2006; accepted 21 November 2006

Abstract—The synthesis and enantioseparation of chiral 3,4-dihydro-1,2,4-benzothiadiazine 1,1-dioxide derivatives are reported herein. A HPLC stopped-flow procedure was applied to the determination of rate constants and free energy barriers of enantiomerization of the compounds synthesized in the presence of achiral stationary phase. The individual enantiomers of the studied compounds were isolated in parallel by preparative HPLC on a Chiraspher NT column. Rate constants and free energy barriers of enantiomerization were determined in the mobile phase. The results were used to determine the influence of the chiral stationary phase on the enantiomerization process.

1. Introduction

Benzothiadiazines have been shown to be potential drugs for memory and cognition disorders, such as attention disorders in children and senile dementias, including early stage Alzheimer diseases.[1] In particular, IDRA21 (±)-**1** [(±)-7-chloro-3-methyl-3,4-dihydro-2*H*-1,2,4-benzothiadiazine 1,1-dioxide] (Fig. 1) was shown to be a potent cognition enhancer in animals suggesting the potential applicability of this drug as a nootropic agent.[2–6]

Like other chiral cognition enhancers of the benzothiadiazine type, IDRA21 contains a stereogenic carbon atom in the benzothiadiazine ring.

Previously, we have reported the resolution of IDRA21 enantiomers by liquid chromatography on an optically active column and found that a rapid interconversion (enantiomerization) of the IDRA21 enantiomers occurred in aqueous solution.[7] A procedure for the determination of apparent rate constants, and apparent free energy barriers of enantiomerization without the implementation of computer simulation has recently been developed.[8–21] The

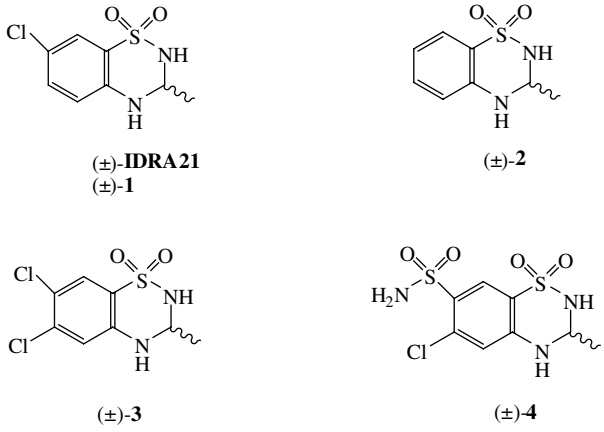

Figure 1. Structures of analytes investigated.

HPLC stopped-flow procedure developed was applied to study on column enantiomerization of (+)-**1** and (−)-**1** and gave a relatively low activation barrier of enantiomerization in aqueous solvents.[8]

To gain further insight in understanding the enantiomerization mechanism of chiral 3,4-dihydro-1,2,4-benzothiadizine 1,1-dioxide type compounds, the on column HPLC stopped-flow procedure developed was applied to study

* Corresponding author. Tel.: +39 059 2055013; fax: +39 059 2055750; e-mail addresses: cannazza.giuseppe@unimore.it; cannazza.giuseppe@unimo.it

0957-4166/$ - see front matter © 2006 Elsevier Ltd. All rights reserved.
doi:10.1016/j.tetasy.2006.11.035

the enantiomerization of three selected chiral compounds: (±)-3-methyl-3,4-dihydro-2*H*-1,2,4-benzothiadiazine 1,1-dioxide (±)-**2**, (±)-6,7-dichloro-3-methyl-3,4-dihydro-2*H*-1,2,4-benzothiadiazine 1,1-dioxide (±)-**3** and (±)-6-chloro-3-methyl-3,4-dihydro-2*H*-1,2,4-benzothiadiazine-7-sulfonamide 1,1-dioxide (±)-**4** (Fig. 1).

Subsequently, the individual enantiomer of (±)-**2**, (±)-**3** and (±)-**4** was isolated by collecting the respective peak fractions of HPLC runs employing conditions where no racemization took place, followed by the determination of rate constants and free energy barriers of enantiomerization in the same solvents used for the on column enantiomerization. These results were used to investigate the influence of substitution at the C(6) and C(7) positions of the benzothiadiazine ring on enantiomerization barriers and to evaluate the influence of the chiral stationary phase (CSP) on the enantiomerization process.

2. Results and discussion

The results of the analytical enantioseparations of (±)-**2**, (±)-**3** and (±)-**4** on Chiralcel OD-R columns are listed in Table 1. Baseline resolutions without racemization were obtained at $t = 0$ °C with the above column.

The enantiomeric nature of eluates was confirmed by circular dichroism indicating, similar to (±)-IDRA21, the (−)-enantiomers eluates before the (+)-enantiomers for all three compounds under investigations.

The on column HPLC stopped-flow procedure previously developed was used to study the enantiomerization of (±)-**2**, (±)-**3** and (±)-**4**. As shown in Figure 2, an experimental protocol of a sequence of three steps was followed. In step 1, the racemic mixture was injected onto the column and enantiomers began to separate. After a specific time, the mobile phase flow was stopped. Racemization of the individual enantiomers occurred in step 2 during column heating at the desired temperature for a time interval set: *E*-(−)-enantiomer was partially converted into *E*-(+)-enantiomer, conversely the *E*-(+)-enantiomer was also transformed into *E*-(−)-enantiomer. In step 3 the column was cooled down to the original low temperature, where practically no racemization occurred and the enantiomer separation could be completed.

The outcome of this protocol resulted in the presence of four peaks in the chromatograms: peaks 1° and 4° belong to the signals of the enantiomer separation of step 1, while the peaks 2° and 3° belong to the signals corresponding to the portion of the interconverted sample corresponding to step 2. Thus it was possible to calculate k_1^{app} and k_{-1}^{app} and apparent free energy barriers of enantiomerization ($\Delta G^{\#app}$) from the individual chromatographic peak areas, which are a weighted means of the different enantiomerization rates in the mobile phase and on the stationary phase.

The resulted k_1^{app} and k_{-1}^{app} and associated free energies of enantiomerization ($\Delta G_1^{\#app}$ and $\Delta G_{-1}^{\#app}$) for the individual enantiomers of (±)-**2** and (±)-**3** are listed in Table 2.

As can be seen, the interconversion rates of the forward and reverse reaction of (±)-**2** and (±)-**3** are practically the same. This result was quite expected as small values of separation factors (α) of the (±)-**2** and (±)-**3** enantiomers were obtained at 40 °C on a Chiralcel OD-R column.

The mean value of energy of enantiomerization for (±)-**2** was about 7 kJ/mol greater than for (±)-**3**, indicating that the chlorine substitution at C(6) and C(7) inhibited enantiomerization.

No (±)-**4** enantiomerization occurred on the Chiralcel OD-R column at 40 °C for 30 min, indicating an energy of enantiomerization greater than 100 kJ/mol.

The individual enantiomers of (±)-**2**, (±)-**3** and (±)-**4**, isolated by semipreparative HPLC on a Chirasphere NT column (Table 1) (Fig. 3), were used to determine the enantiomerization rate constants k^m and the associated energy barriers of enantiomerization ($\Delta G^{\#m}$) at the same temperature and in the same solvent used for the on column enantiomerization. The results are listed in Table 3.

Energy of enantiomerization for (±)-**4** was about 6 kJ/mol greater than for (±)-**3** and about 14 kJ/mol greater than for (±)-**2**.

Moreover, it was possible to calculate the forward (k_1^s) and backward (k_{-1}^s) rate constants of enantiomerizations and the relative energy barriers of enantiomerization ($\Delta G_1^{\#s}$ and $\Delta G_{-1}^{\#s}$) for (±)-**2** and (±)-**3** enantiomers in the chiral environment of CSP from k_1^{app}, k_{-1}^{app} and k^m according to the following equations:

$$k_1^{app} = \frac{1}{1 + k_{(-)}^{enant}} k^m + \frac{k_{(-)}^{enant}}{1 + k_{(-)}^{enant}} k_1^S \quad (1)$$

$$k_{-1}^{app} = \frac{1}{1 + k_{(+)}^{enant}} k^m + \frac{k_{(+)}^{enant}}{1 + k_{(+)}^{enant}} k_{-1}^S \quad (2)$$

Table 1. Chromatographic enantioseparations of (±)-**2**, (±)-**3** and (±)-**4**

Compounds	Chiralcel OD-R[a]				Chiraspher NT[b]			
	$k'_{(-)}$	$k'_{(+)}$	α	R_S	$k'_{(+)}$	$k'_{(-)}$	α	R_S
(±)-**2**	6.92	9.59	1.39	1.92	8.91	7.73	1.15	1.86
(±)-**3**	16.52	19.19	1.64	1.64	6.18	5.27	1.17	1.54
(±)-**4**	8.36	11.69	1.40	1.59	19.43	17.52	1.11	1.62

[a] Column Chiralcel OD-R; mobile phases: water/acetonitrile 70:30 (v/v) for (±)-**2** and (±)-**3**, water/acetonitrile 50:50 (v/v) for (±)-**4**; $t = 0$ °C; flow: 0.5 ml/min for (±)-**2** and (±)-**3**, 0.7 ml/min for (±)-**4**.

[b] Column Chiraspher NT; mobile phase: hexane/tetrahydrofurane 70:30 (v/v); $t = 25$ °C; flow: 3 ml/min.

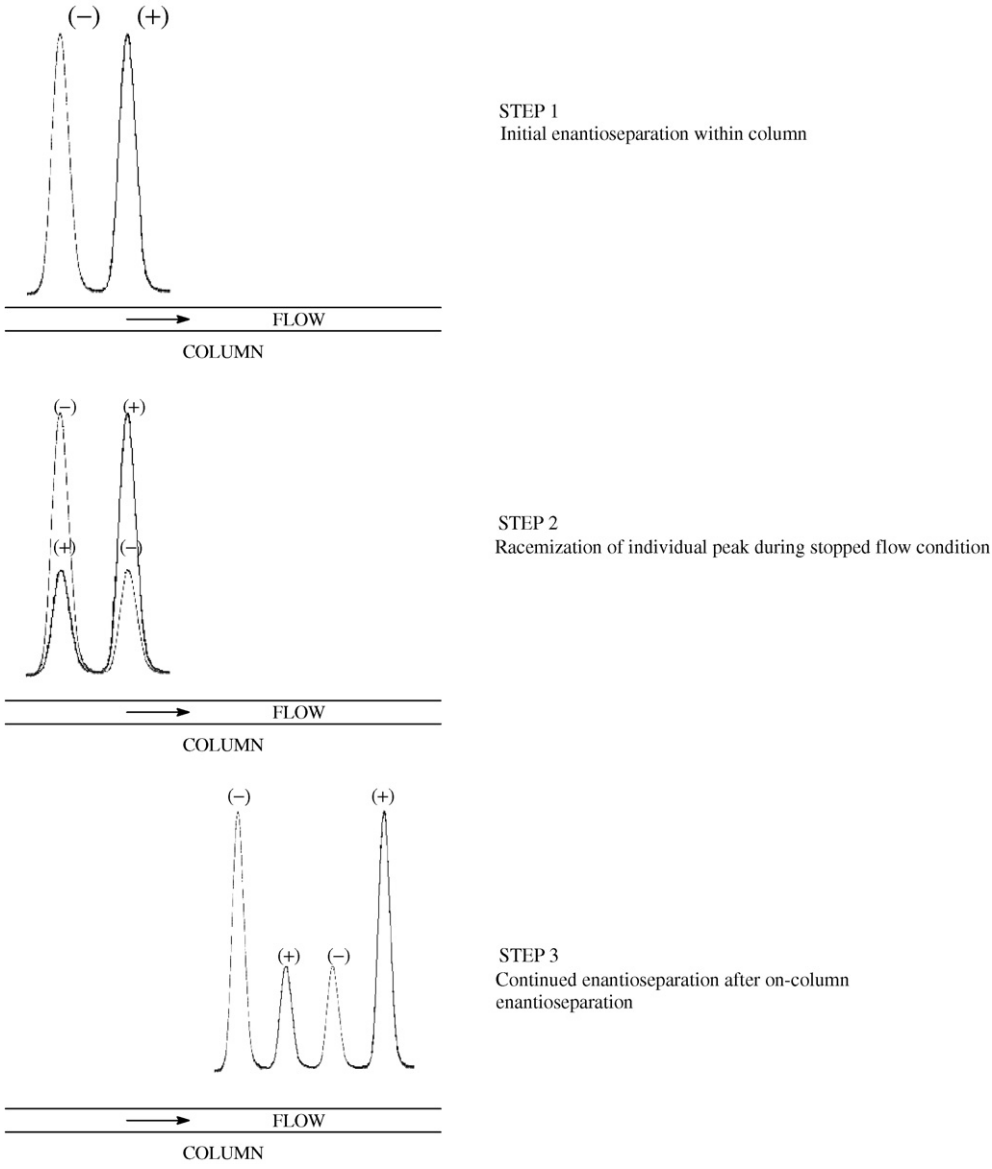

Figure 2. Computer simulated concept of on-column enantiomerization to be investigated by stopped-flow technique during chromatographic enantioseparation of studied compounds. Step 1. Compound was injected and a partial elution of enantiomers occurred at low temperature conditions. Step 2. The mobile phase flow was stopped and the column was kept for a set time at a set higher temperature. Each enantiomer racemized in a time- and temperature-dependent manner. Step 3. The column was cooled back to the initial temperature and the original flow rate was reinforced, leading to enantiomer separation.

Table 2. On-column enantiomerization of (±)-**2**, (±)-**3**

Compound	Eluents	k_1^{app} (s^{-1})	k_{-1}^{app} (s^{-1})	$\Delta G_1^{\#\,app}$ (KJ/mol)	$\Delta G_{-1}^{\#\,app}$ (kJ/mol)	t (°C)
2	Water/acetonitrile 80:20 (v/v)	$1.45\times10^{-3}\pm0.45\times10^{-3}$	$1.11\times10^{-3}\pm0.05\times10^{-3}$	93.75 ± 0.71	94.43 ± 0.10	40
3	Water/acetonitrile 60:40 (v/v)	$1.29\times10^{-4}\pm0.13\times10^{-4}$	$1.20\times10^{-4}\pm0.12\times10^{-4}$	99.06 ± 0.57	98.31 ± 0.54	40

Column: Chiralcel OD-R (25 × 0.46 cm ID, 10 μm) tris(3,5-dimethylphenyl-carbamate); flow rate: 0.5 ml/min, column operation temperature = 12 °C, $n = 4$; time intervals for on-column enantiomerization at 40° = 5′, 10′, 15′, 22.5′.

where $k_{(-)}^{enant}$ and $k_{(+)}^{enant}$ are the retention factors of the (−)- and (+)-enantiomers, respectively.

The results showed that the interactions of the enantiomers with the CSP have an inhibitory effect on enantiomerization being $\Delta G_1^{\#s}$ and $\Delta G_{-1}^{\#s}$ greater than $\Delta G^{\#m}$ (Table 3).

The differences between the energies of enantiomerization in the mobile phase and in the CSP increase with the retentions of analytes (Table 4).

The finding that the complexation of enantiomers with the CSP increased the enantiomerization barrier was expected,

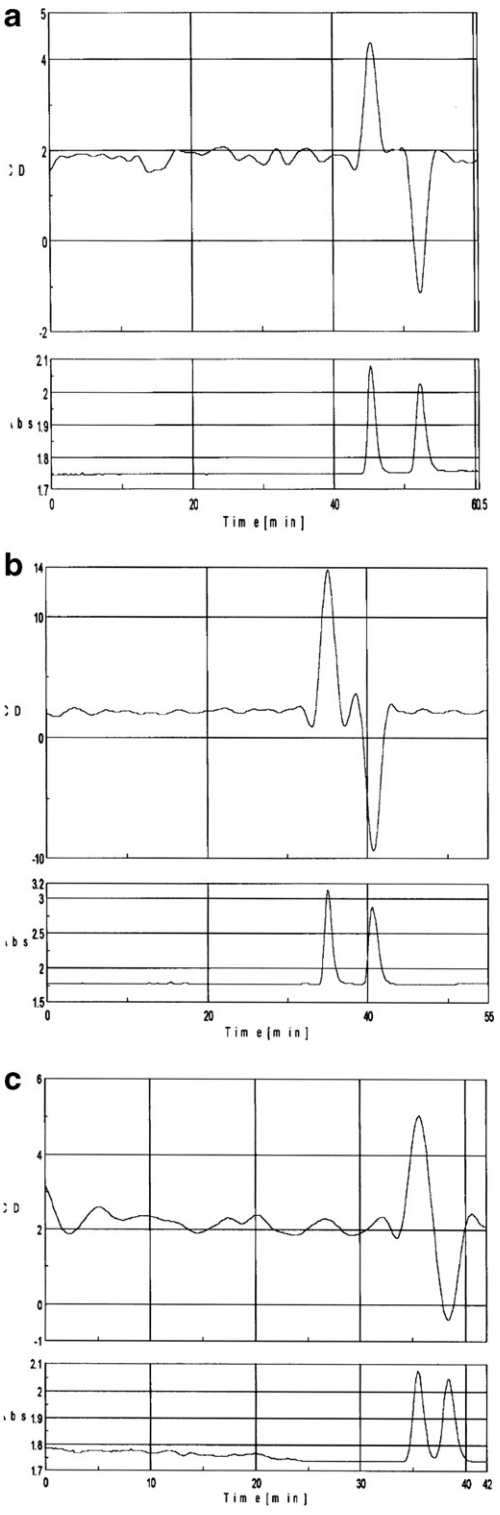

Figure 3. Chromatographic resolution of (a) (±)-3-methyl-3,4-dihydro-2*H*-1,2,4-benzothiadiazine 1,1-dioxide (±)-**2**, (b) (±)-6,7-dichloro-3-methyl-3,4-dihydro-2*H*-1,2,4-benzothiadiazine 1,1-dioxide (±)-(**3**), (c) (±)-6-chloro-3-methyl-3,4-dihydro-2*H*-1,2,4-benzothiadiazine-7-sulfonamide 1,1-dioxide (±)-**4** on Chiraspher NT column monitored by absorption (below) and circular dichroism (CD) detection (above). Eluent: hexane: tetrahydrofurane 70:30 (v/v); $t = 25$ °C; flow: 3 ml/min.

as interactions with the CSP may have to be broken to reach the transition state.

3. Experimental

The chromatographic apparatus consisted of Jasco PU-980 intelligent Pump, and a 7125 Reodhyne manual injector equipped with a 20 μl or 200 μl sample loop. A model Jasco J-710 spectropolarimeter or a UV a Jasco 875-UV was used as a detector. Chromatograms were recorded with J-700 system program or a Spectra Physics Integrator. A 7000 Reodhyne valve installed in a post column mode permitted the trapping of peak fractions for the acquisition of CD and UV spectra with an on-line installed spectropolarimeter detector. Column temperature regulation was achieved by a thermostated water bath Haake F3. The columns used were a Chiralcel OD-R column (cellulose tris-3,5-dimethylphenylcarbammate; 250 × 4.6 mm ID; 10 μm) purchased from Daicel and a Chiraspher NT (poly(*N*-acryloyl-*S*-phenylalaninethylester); 250 × 4 mm. ID; 5 μm) purchased from Merck.

Melting points were determined with an Electrothermal apparatus and are uncorrected. IR spectra were recorded on a Perkin Elmer Model 1600 FT-IR spectrometer (KBr pellets) and were consistent with the assigned structures. ^{1}H NMR spectra were recorded with a Brucker DPX 200 spectrometer using DMSO-d_6 as solvent and tetramethylsilane (TMS) as the external standard. Chemical shifts (δ) are in parts per million and coupling constants (J) in hertz. Multiplicities are abbreviated as follows: s, singlet; d, doublet; dd, double doublet, m, multiplet. Elemental analyses were performed on a Carlo Erba Elemental Analyzer Model 1106 apparatus and the results are within ±0.4% of the theoretical values.

3.1. Chemistry

3.1.1. General procedure for the synthesis of derivatives 2–4. A solution of 20 mmol of the corresponding benzenesulfonamide in dioxane, containing 1.1 equiv of acetaldehyde and few drops of concentrated H_2SO_4, was heated at reflux for 3 h. The solvent was evaporated and the crude was crystallized from acetone/petroleum benzine at a temperature of 90–100 °C.[22]

3.1.2. (±)-3-Methyl-3,4-dihydro-2*H*-1,2,4-benzothiadiazine 1,1-dioxide (±)-2. Yield: 92%, mp 212–213 °C, ^{1}H NMR (DMSO-d_6) $\delta = 1.44$ (d, $J = 6.2$, 3H), $\delta = 4.76$–4.91 (m, 1H), $\delta = 6.67$–6.75 (m, 1H), $\delta = 6.77$ (dd, 1H, $J = 0.6$; 0.8), $\delta = 7.08$ (s, 1H), $\delta = 7.25$–7.33 (m, 1H), $\delta = 7.43$ (d, 1H, $J = 11.9$), $\delta = 7.45$ (dd, 1H, $J = 1.4$; 11.9).

3.1.3. (±)-6,7-Dichloro-3-methyl-3,4-dihydro-2*H*-1,2,4-benzothiadiazine 1,1-dioxide (±)-3. Yield: 91%, mp 222–225 °C, ^{1}HNMR (DMSO-d_6) $\delta = 1.42$ (d, $J = 6.2$, 3H), $\delta = 4.75$–4.90 (m, 1H), $\delta = 7.00$ (s, 1H), $\delta = 7.49$ (s, 1H), $\delta = 7.66$ (s, 1H), $\delta = 7.45$ (d, 1H, $J = 1.4$; 11.7).

3.1.4. (±)-6-Chloro-3-methyl-3,4-dihydro-2*H*-1,2,4-benzothiadiazine-7-sulfonamide 1,1-dioxide (±)-4. Yield: 44%, mp 238–240 °C, ^{1}H NMR (DMSO-d_6) $\delta = 1.45$ (d, $J = 6.2$, 3H), $\delta = 4.85$–4.94 (m, 1H), $\delta = 6.93$ (s, 1H), $\delta = 7.45$ (s, 2H), $\delta = 7.80$ (d, $J = 11.6$), $\delta = 7.96$ (s, 1H), $\delta = 7.98$ (s, 1H).

Table 3. Calculated values of enantiomerization of IDRA21 on OD-CSP

Compound	Solvents	K_1^s (s^{-1})	K_{-1}^s (s^{-1})	$\Delta G_1^{\#s}$ (kJ/mol)	$\Delta G_{-1}^{\#s}$ (kJ/mol)	Temperatures (°C)
2	Water/acetonitrile 80:20 (v/v) (flow 0.5 ml/min)	$4.93\times10^{-4}\pm2.62\times10^{-4}$	$6.95\times10^{-5}\pm8.13\times10^{-6}$	96.55 ± 1.10	101.64 ± 0.29	40
3	Water/acetonitrile 70:30 (v/v) (flow 0.5 ml/min)	$6.90\times10^{-5}\pm1.68\times10^{-5}$	$8.13\times10^{-5}\pm1.59\times10^{-5}$	101.72 ± 0.57	101.29 ± 0.46	40

k_1^s and k_{-1}^s were calculated according to Eqs. 1 and 2.

Table 4. Off-column enantiomerization of (±)-(**2**), (±)-(**3**), (±)-(**4**) enantiomers in water/acetonitrile

Compound	Solvents	k_1^m (s^{-1})	k_{-1}^m (s^{-1})	$\Delta G_1^{\#m}$ (kJ/mol)	$\Delta G_{-1}^{\#m}$ (kJ/mol)	t (°C)
2	Water/acetonitrile 80:20 (v/v)	$3.65\times10^{-3}\pm0.12\times10^{-3}$	$4.20\times10^{-4}\pm0.42\times10^{-4}$	91.34 ± 0.10	90.98 ± 0.25	40
3	Water/acetonitrile 70:30 (v/v)	$6.36\times10^{-4}\pm0.54\times10^{-4}$	$6.39\times10^{-4}\pm0.63\times10^{-4}$	95.84 ± 0.21	95.88 ± 0.24	40
4	Water/acetonitrile 70:30 (v/v)	$3.31\times10^{-4}\pm0.11\times10^{-4}$	$2.54\times10^{-4}\pm0.04\times10^{-4}$	103.99 ± 0.09	104.73 ± 0.05	60

Column: Chiralcel OD-R (25 × 0.46 cm ID, 10 μm) tris(3,5-dimethylphenyl-carbamate); flow rate: 0.5 ml/min, column operation temperature = 12 °C, $n = 4$; time intervals for on-column enantiomerization at 40° = 5′, 10′, 15′, 22.5′.

3.2. Chromatographic enantioseparations

Enantioseparation of (±)-IDRA21, (±)-**2** and (±)-**3** was carried out isocratically at different temperatures. The mobile phases consisted of hexane and 2-propanol for Chiralcel OD column, water and acetonitrile for Chiralcel OD-R column and hexane and tetrahydrofurane (THF) for Chiraspher NT column. The compounds were dissolved in 2-propanol, acetonitrile or THF depending on the column system used, while sample solutions were passed through a 0.45 μm filter prior to injection. The detectors were set at 254 nm. Pure enantiomers of IDRA21, **2** and **3** were obtained using a Chiraspher NT column and fraction collection of respective peaks. The mobile phases (hexane and THF) were evaporated by a stream of nitrogen at room temperature. The enantiomeric excess of the collected enantiomers was monitored on the same Chiraspher NT column.

3.3. On-column enantiomerization

As shown in Figure 2, a racemic mixture of IDRA21 was first injected on column, kept at low temperature and passed through it for a fixed period of time. After this time, the mobile phase flow was stopped and the column was kept at a certain temperature for a set period of time to effect enantiomerization of the separated individual enantiomers of IDRA21. Afterwards, the column was cooled back to the initial low temperature conditions and continued to run at the original flow rate. Apparent enantiomerization rates were calculated using the peak areas of separated enantiomers, as depicted in Figure 2.

3.4. Off-column enantiomerization

Single enantiomers of IDRA21, **2** and **3**, obtained as previously described by low temperature chromatography and solvent evaporation, were used to study enantiomerization in different solvents. These enantiomers (~20 μg) were dissolved in the individual solvent and thermostated in a thermostated bath. Enantiomerizations were monitored by chromatography on Chiralcel OD or OD-R columns of samples fractions (20 μl) every 5 min for at least four times. Enantiomeric ratios were calculated by measuring the peaks areas of the enantiomers.

References

1. Wyklicky, L.; Patneau, D. K.; Mayer, M. L. *Neuron* **1991**, *7*, 971–984.
2. Patneau, D. K.; Wyklicky, L.; Mayer, M. L. *J. Neurosci.* **1993**, *13*, 3496–3509.
3. Yamada, K. A.; Tang, C. M. *J. Neurosci.* **1993**, *1*, 3904–3915.
4. Bertolino, M.; Baraldi, M.; Parenti, C.; Braghiroli, D.; Di Bella, M.; Vicini, S.; Costa, E. *Recept. Chan.* **1993**, *1*, 267–278.
5. Uzunov, D. P.; Zivkovich, I.; Pirkle, W. H.; Costa, E.; Guidotti, A. *J. Pharm. Sci.* **1995**, *84*, 937–942.
6. Zvkovic, I.; Thompson, D. M.; Bertolino, M.; Uzunov, D.; Di Bella, M.; Costa, E.; Guidotti, A. *J. Pharmacol. Exp. Ther.* **1995**, *2*, 300–309.
7. Impagniatiello, F.; Oberto, A.; Longone, P.; Costa, E.; Guidotti, A. *Proc. Natl. Acad. Sci. U.S.A.* **1997**, *94*, 7053–7058.
8. Cannazza, G.; Braghiroli, D.; Baraldi, M.; Parenti, C. *J. Pharm. Biom. Anal.* **2000**, *23*, 117–125.
9. Cannazza, G.; Braghiroli, D.; Tait, A.; Baraldi, M.; Parenti, C.; Lindner, W. *Chirality* **2001**, *13*, 94–101.
10. Eliel, E. L.; Wilen, S. H. *Stereochemistry of Organic Compounds*; John Wiley & Sons: New York, 1994; pp 424–426.
11. Reist, M.; Testa, B.; Carrupt, P. A.; Jung, M.; Schurig, V. *Chirality* **1995**, *7*, 396–400.
12. Jung, M.; Schurig, V. *J. Am. Chem. Soc.* **1992**, *114*, 529–534.
13. Mannschreck, A.; Zimmer, H.; Pustet, N. *Chimia* **1989**, *43*, 165–166.
14. Cabrera, K.; Jung, M.; Fluck, M.; Schurig, V. *J. Chromatogr. A* **1996**, *731*, 315–321.
15. Burkle, W.; Karfunkel, H.; Schurig, V. *J. Chromatogr.* **1984**, *288*, 1–14.
16. Trapp, O.; Schurig, V. *J. Am. Chem. Soc.* **2000**, *122*, 1424–1430.
17. Weseloh, G.; Wolf, C.; Konig, W. A. *Angew. Chem.* **1995**, *107*, 1771–1772.
18. Schurig, V.; Glausch, A.; Fluck, M. *Tetrahedron: Asymmetry* **1995**, *6*, 2161–2164.
19. Lorenz, K.; Yashima, E.; Okamoto, Y. *Angew. Chem., Int. Ed.* **1998**, *110*, 2025–2028.
20. Tobler, E.; Lammerhofer, M.; Mancini, G.; Lindner, W. *Chirality* **2001**, *13*, 641–647.
21. Krupcik, J.; Oswald, P.; Májek, P.; Sandra, P.; Armstrong, D. W. *J. Chromatogr. A* **2003**, *1000*, 779–800.
22. Braghiroli, D.; Puia, G.; Cannazza, G.; Tait, A.; Parenti, C.; Losi, G.; Baraldi, M. *J. Med. Chem.* **2002**, *45*, 2355–2357.